*International Journal of Innovative Computing, Information and Control*
Volume **19**, Number **4**, August **2023**

pp. 1195–1208

# PRESCRIBED-PERFORMANCE-BASED ADAPTIVE NEURAL BACKSTEPPING CONTROL FOR PERMANENT MAGNET LINEAR SYNCHRONOUS MOTOR

Li Zhang[1], Jinlei Pei[2,*], Tinglong Pan[2], Weilin Yang[2] and Dezhi Xu[2]

[1]School of Automation
Nanjing Institute of Technology
No. 1, Hongjing Avenue, Jiangning District, Nanjing 211167, P. R. China
zdhxzli@njit.edu.cn

[2]School of Internet of Things Engineering
Jiangnan University
No. 1800, Lihu Avenue, Wuxi 214122, P. R. China
{ tlpan; wlyang; xudezhi }@jiangnan.edu.cn
*Corresponding author: 7221905014@stu.jiangnan.edu.cn

Received November 2022; revised February 2023

Abstract. *A new control strategy based on neural network backstepping and a prescribed performance function is proposed for speed control in the permanent magnet linear synchronous motor (PMLSM) systems. First, the prescribed performance function is introduced to transform the control error and improve the dynamic and static performance of the system. This limits the error tracking of the original system to prescribed bounds if the transformed system is stable. Then, the disturbance observer is designed with radial basis function neural network and introduced into the controller as compensation signal. Considering the differential expansion problem in the backstepping control, the output of the controller is filtered by the command filter. This filtered output is then used in feed forward compensation, further improving system performance. Finally, the control scheme is verified by a motor experiment platform. According to the experimental results, it is proved that the control strategy can improve the robustness of the system and the ability to suppress disturbances.*
**Keywords:** Prescribed performance control, Disturbance observer, Constrained command filter, Permanent magnet linear synchronous motor

1. **Introduction.** In recent years, permanent magnet linear synchronous motor (PMLSM) has become widely used because of its good control performance and efficiency [1,2]. Applications include urban rail transit, high-precision machine tools and some automatic control fields [3,4]. In contrast with rotary motors, PMLSM has simple mechanical structures, high acceleration and good dynamic performance [5,6]. However, due to the structural characteristics of the PMLSM, its performance will be affected by the system uncertainties such as the change of mover mass, inevitable friction force, ripple force, end effect and external load disturbance [7-9]. In order to ensure the accuracy and stability of motion tracking, it is necessary to overcome these uncertainties in the design of the controller [10].

In order to suppress the influence of disturbances in system control, various control strategies have been proposed for nonlinear systems, such as adaptive backstepping control (ABC) [11,12], sliding mode control (SMC) [13,14] and neural network control (NNC) [15,16]. Backstepping control is a common control strategy for nonlinear systems which

DOI: 10.24507/ijicic.19.04.1195

can be combined with other algorithms to make up for its shortcomings. In [17], the adaptive command filter backstepping control method has been proposed to track the position of the linear motor. However, this method cannot compensate for the disturbance in the system. In [18], neural network observer was used to observe the unknown disturbance of the system. This method obtains the uncertain parameters of the system through the universal function approximation, but the performance of quantities such as error, convergence rate and overshoot during transient tracking cannot be preset by design [19,20]. In [21], aiming at a class of uncertain nonlinear strict-feedback systems with actuator fault, an adaptive fuzzy fault-tolerant control scheme has been proposed. However, this method cannot improve the dynamic response.

To ensure output error convergence to a predetermined small range, a prescribed performance control (PPC) method is proposed. The key to PPC is to obtain a conversion error from the actual system through a prescribed performance function (PPF) [22,23]. The PPF is the bound of system error. The conversion error is then introduced into the design of the controller. If the error after conversion is bounded, the error of the original system is within the prescribed bound. The prescribed performance control method has been successfully applied in wide range nonlinear systems such as surface vessels, active suspension systems and servo systems [24-26].

In this paper, a prescribed performance based adaptive neural backstepping is proposed for PMLSM control, and the prescribed performance function is introduced for limiting the tracking error. The differential expansion and input saturation in the backstepping control are compensated by the command filter. Experimental results in dSPACE demonstrate the proposed strategy has good steady and dynamic performance. The main contributions of this paper are reflected as follows:

1) To improve the dynamic response, the prescribed performance function is introduced for limiting the tracking error in this paper;

2) In contrast with the existing results, the control method proposed in this paper can control the state error to converge in finite time, improve the response speed of the system and eliminate the tracking error;

3) The neural network observer is used in this paper, which can effectively compensate the external interference of the system and improve the stability of the system.

The remainder of this article is organized as follows. Section 2 analyzes the model of PMLSM, gives the structure of PMLSM and deduce the equation of motion of PMLSM. Section 3 describes the method of the controller design, designs the backstepping control and the disturbance observer based on RBFNN. The proposed method is verified by experiments and compared with the experimental results produced by PI and ABC control methods in Section 4. Finally, we give a summary of the proposed method and indicate some further research directions in Section 5.

2. **Mathematical Model of PMLSM.** Figure 1 shows the structure diagram of PMLSM. It can be seen as a permanent magnet synchronous motor (PMSM) cut open and unfolded. It is composed of a primary that contains moving windings and a secondary that contains permanent magnet. At present, vector control is mainly carried out in $d$-$q$ rotating coordinate system. On the basis of neglecting flux distortion and eddy current loss, the voltage model of PMLSM in $d$-$q$ coordinates can be written as

$$u_d = Ri_d + L_d\frac{di_d}{d_t} - v\frac{\pi n_p}{\tau}L_d i_q \tag{1}$$

$$u_q = Ri_q + L_q\frac{di_q}{d_t} + v\frac{\pi n_p}{\tau}\left(L_q i_d + \psi_f\right) \tag{2}$$

where $u_d$, $u_q$ represent voltages of $d$-$q$ axis, $i_d$, $i_q$ represent current of $d$-$q$ axis, $\tau$ is the pole pitch, $\pi$ is the circular constant, $L_d$, $L_q$ are the inductance of $d$-$q$ axis, $R$ is the stator resistance, $v$ is the linear motor speed, and $\psi_f$ is the permanent magnet flux. Because the mutual inductance of linear motor caused by side effect is small, it can be ignored in general control systems. When the mutual inductance is ignored, the equation of electromagnetic thrust is obtained as follows

$$F_e = \frac{3\pi}{2\tau} n_p \psi_f i_q \tag{3}$$

where $F_e$ is the electromagnetic thrust and $n_p$ is the pole pair of linear motor. Therefore, the mechanical dynamic equation is expressed as

$$F_e = M\frac{dv}{dt} + Bv + F \tag{4}$$

$$F = F_l + F_f + F_d \tag{5}$$

where $M$ represents the total mass of the mover, $B$ is the viscous friction coefficient, and $F$ is the total uncertainty of the system, that is, load disturbances $F_l$, friction forces $F_f$ and force ripple caused by end effect $F_d$.

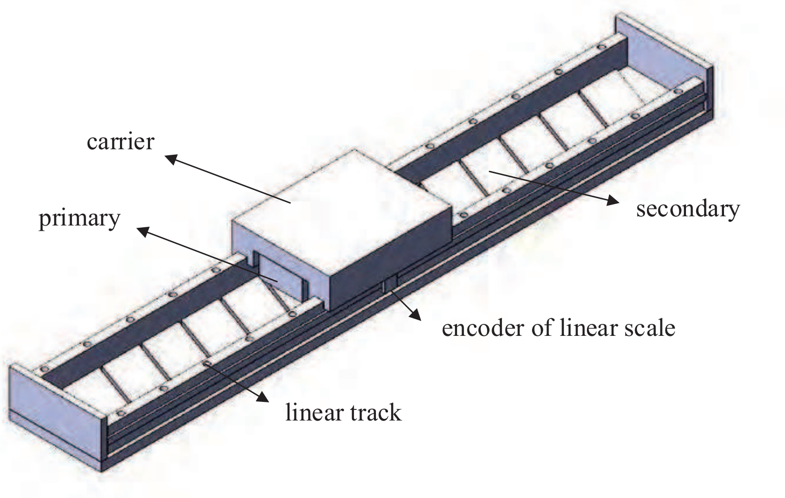


FIGURE 1. System control block diagram

Considering the influence of external factors, the simplified motor motion equation is obtained as follows

$$\begin{cases} \dfrac{dv}{dt} = \dfrac{3\pi n_p \psi_f}{2\tau M} i_q - \dfrac{Bv}{M} + F \\ \dfrac{di_q}{dt} = \dfrac{u_q}{L_q} - \dfrac{v\pi n_p \psi_f}{L_q \tau} - \dfrac{v\pi n_p i_d}{\tau} - \dfrac{R}{L_q} i_q \\ \dfrac{di_d}{dt} = \dfrac{u_d}{L_d} + \dfrac{\pi n_p v i_q}{\tau} - \dfrac{R i_d}{L_d} \end{cases} \tag{6}$$

3. **Controller Design.** In this section, combined with the prescribed performance function and the neural network observer, an adaptive backstepping controller is designed to improve the tracking performance of the system.

3.1. **Prescribed performance function.** In order to constrain the speed tracking error of PMLSM to a given range, we introduce the performance function $\mu(t)$ as prescribed performance bound. $\mu(t)$ in this paper is selected as

$$\mu(t) = (\mu_0 - \mu_\infty)\exp(-at) + \mu_\infty \tag{7}$$

where $\mu_0 > \mu_\infty > 0$, and $a$ is a positive constant. Based on prescribed performance functions, the original tracking error of the system can be rewritten as follows:

$$\begin{cases} -d\mu(t) < e(t) < \mu(t), & e(0) \geq 0 \\ -\mu(t) < e(t) < d\mu(t), & e(0) < 0 \end{cases} \tag{8}$$

where $e(t)$ is a tracking error, and $0 \leq d \leq 1$.

To transform (8) into an equivalent unconstrained one, a smooth increasing function $S(\varepsilon)$ and transformed error $\varepsilon$ are introduced. The function has the following characteristics:

1) $\begin{cases} -d < S(\varepsilon) < 1, & e(0) \geq 0 \\ -1 < S(\varepsilon) < d, & e(0) < 0 \end{cases}$

2) $\begin{cases} \lim\limits_{\varepsilon\to+\infty} S(\varepsilon) = -d \lim\limits_{\varepsilon\to-\infty} S(\varepsilon) = -1, & e(0) \geq 0 \\ \lim\limits_{\varepsilon\to+\infty} S(\varepsilon) = 1 \lim\limits_{\varepsilon\to-\infty} S(\varepsilon) = d, & e(0) < 0 \end{cases}$

Therefore, the function $S(\varepsilon)$ is selected as

$$S(\varepsilon) = \begin{cases} \dfrac{\exp(\varepsilon) - d\exp(-\varepsilon)}{\exp(\varepsilon) + \exp(-\varepsilon)}, & e(0) \geq 0 \\ \dfrac{d\exp(\varepsilon) - \exp(-\varepsilon)}{\exp(\varepsilon) + \exp(-\varepsilon)}, & e(0) < 0 \end{cases} \tag{9}$$

From the properties of $S(\varepsilon)$, $e(t)$ can be expressed as follows:

$$e(t) = \mu(t)S(\varepsilon) \tag{10}$$

$$\varepsilon = S^{-1}[e(t)/\mu(t)] \tag{11}$$

Note that in the prescribed performance function, all the associated parameters are priori designed. For any initial condition $e(0)$, as long as (8) is satisfied, $\varepsilon$ can be controlled to be bounded. Thus, the boundary control of a system with original error is transformed into a stabilization control of a system respect to $\varepsilon$. Motivated by (11), the simplified conversion function is proposed as follows [28]:

$$\varepsilon = \begin{cases} \dfrac{1}{2}\ln\dfrac{\lambda(t) + d}{1 - \lambda(t)}, & e(0) \geq 0 \\ \dfrac{1}{2}\ln\dfrac{\lambda(t) + 1}{d - \lambda(t)}, & e(0) < 0 \end{cases} \tag{12}$$

where $\lambda(t) = e(t)/\mu(t)$.

3.2. **Design of disturbance observer.** Disturbance observer is designed by radial basis function neural network (RBF NN), and the observed results are used in the controller as compensation signals to counteract unknown disturbances.

In RBF NN, the input vector is selected as $x = [x_1, x_2, x_3, \ldots, x_n]$. Hidden layer consists of a number of neurons. The output of the hidden layer is $h = [h_1, h_2, h_3, \ldots, h_m]$, and $h_j$ is the output of the $j$th neuron. Gaussian function is adopted as

$$h_j(x, c, b) = \exp\left(-\frac{\|x - c_j\|^2}{2b_j^2}\right) \quad j = 1, 2, \ldots, m \tag{13}$$

where $j$ is the node in the hidden layer of the network, $b_j = [b_1, b_2, \dots, b_m]^T$ is the standard deviation of the RBF NN, $c_j = [c_{j1}, c_{j2}, \dots, c_{jn}]$ is the coordinate vector at the center of the $j$th neuron function [27].

The output of RBF NN is calculated by adding weight. Node output is

$$f(x) = \sum_{j=1}^{m} W_{ji} h_j(x, c, b), \quad i = 1, 2, \dots, n \tag{14}$$

where $W_{ji}$ is the adaptive connection weight of the $j$th hidden node to the $i$th output.

In the proposed neural network observer, the input signal is the speed tracking error vector $[e_1, \dot{e}_1]$, and the signal of output layer is utilized to approximate the disturbance $F$. According to the approximation theory, the optimal approximation $F$ can be described as

$$F = f(x) - \delta = W^T h(x) - \delta \tag{15}$$

where $W$ is the ideal weight vector, and $\delta$ is the approximation error. When enough neurons are selected in the neural network, the value of approximation error $\delta$ can be ignored.

The output of the disturbance observer is

$$\hat{F} = \hat{W}^T h(x) \tag{16}$$

where $\hat{W}$ is the estimation of the ideal weight vector $W$.

Noting (15), (16), the optimal approximation $F$ can be expressed as

$$F = \hat{F} + \tilde{W}^T h(x) - \delta \tag{17}$$

where $\tilde{W} = W - \hat{W}$ represents the estimation error of the weight vector.

For permanent magnet synchronous linear motor system, the evaluation function $E$ of neural network is selected as

$$E = \frac{1}{2}(v - v_c)^2 = \frac{1}{2}e_1^2 \tag{18}$$

We can get the central coordinate vector $c_j$ and the standard deviation $b_j$ through gradient descent method.

$$\Delta c_{ij} = -\rho \frac{\partial E}{\partial c_{ij}} = -\rho \frac{\partial E}{\partial \hat{F}} \cdot \frac{\partial \hat{F}}{\partial c_{ij}} = -\rho \frac{\partial E}{\partial \hat{F}} w_j h_j \frac{x_i - c_{ij}}{b_j^2} \tag{19}$$

$$c_{ij}(k+1) - c_{ij}(k) = \Delta c_{ij}(k) + \alpha \left[c_{ij}(k) - c_{ij}(k-1)\right] \tag{20}$$

$$\Delta b_j = -\rho \frac{\partial E}{\partial b_j} = -\rho \frac{\partial E}{\partial \hat{F}} \cdot \frac{\partial \hat{F}}{\partial b_j} = -\rho \frac{\partial E}{\partial \hat{F}} w_j h_j \frac{\|x_i - ci_j\|^2}{b_j^3} \tag{21}$$

$$b_j(k+1) - b_j(k) = \Delta b_j(k) + \alpha \left[b_j(k) - b_j(k-1)\right] \tag{22}$$

where $\rho$ is the learning factor of neural network.

3.3. **Backstepping controller design.** According to the idea of field orientation control, the PMLSM system can be decoupled into speed and current loops. We define the speed and current tracking errors as

$$e_1(t) = v(t) - v^c(t) \tag{23}$$

$$e_2(t) = i_q(t) - i_q^c(t) \tag{24}$$

$$e_3(t) = i_d(t) - i_d^c(t) \tag{25}$$

where $v^c(t)$ is the reference speed, $i_d^c(t)$ is the reference current, $i_q^c(t)$ is the filtered command of $i_q^d(t)$, and the structure of command filter will be presented below. Substituting $v$ into (12), the derivative of $\varepsilon$ can be rewritten as

$$\dot{\varepsilon} = \frac{\partial S^{-1}}{\partial \lambda}\dot{\lambda} = \frac{\partial S^{-1}}{\partial \lambda} \cdot \frac{\dot{e}_1\mu - e_1\dot{\mu}}{\mu^2} = r\left(\dot{e}_1 - \frac{e_1\dot{\mu}}{\mu}\right) \tag{26}$$

where $r = \left(\partial S^{-1}/\partial\lambda\right) \cdot (1/\mu)$ can be calculated by (10). Due to $\left(\partial S^{-1}/\partial\lambda\right) > 0$ and $\mu(t) > 0$, we know $r > 0$.

In order to eliminate the unknown disturbance in the system, we use the observation value $\hat{F}$ obtained by RBF NN to replace the $F$ in the controller. Construct Lyapunov function as

$$V_1 = \frac{1}{2}\varepsilon^2 + \frac{\tilde{W}^T\tilde{W}}{2\gamma} \tag{27}$$

Taking the derivative of $V_1$, one obtains

$$\begin{aligned} \dot{V}_1 &= \varepsilon\dot{\varepsilon} + \frac{\tilde{W}}{\gamma}\dot{\hat{W}} \\ &= \varepsilon r\left(\dot{e}_1 - \frac{e_1\dot{u}}{u}\right) + \frac{\tilde{W}^T}{\gamma}\dot{\hat{W}} \\ &= \varepsilon r\left(\frac{3\pi n_p\psi_f}{2\tau M}i_q - \dot{v}_c - \frac{Bv}{M} + F - \frac{e_1\dot{u}}{u}\right) + \frac{\tilde{W}^T}{\gamma}\dot{\hat{W}} \\ &= \varepsilon r\left(\frac{3\pi n_p\psi_f}{2\tau M}i_q - \dot{v}_c - \frac{Bv}{M} + \hat{F} + \tilde{W}^T h(x) - \frac{e_1\dot{u}}{u}\right) + \frac{\tilde{W}^T}{\gamma}\dot{\hat{W}} \\ &= \varepsilon r\left(\frac{3\pi n_p\psi_f}{2\tau M}i_q - \dot{v}_c - \frac{Bv}{M} + \hat{F} - \frac{e_1\dot{u}}{u}\right) + \tilde{W}^T\left(\frac{\dot{\hat{W}}}{\gamma} - \varepsilon r h(x)\right) \end{aligned} \tag{28}$$

The virtual controller of speed loop can be designed as

$$i_q^d = \frac{2\tau M}{3\pi\psi_f n_p}\left(\frac{Bv}{M} + \dot{v}^c - F + \frac{e_1\dot{\mu}}{\mu} - k_1\frac{\varepsilon}{r}\right) \tag{29}$$

$$\dot{\hat{W}} = \gamma \mathrm{Proj}\left(\hat{W}, \varepsilon r h(x)\right) \tag{30}$$

where $\mathrm{Proj}(\cdot,\cdot)$ represents the projection of adaptive parameters.

In order to ensure that the adaptive parameters are bounded in practical application, the discontinuous projection adaptive law is used to estimate the uncertain parameters of PMLSM. The projection operator is defined as

$$\mathrm{Proj}\left(\hat{\sigma}, x\right) = \begin{cases} 0, & \hat{\sigma} = \hat{\sigma}_{\max} \text{ and } x > 0 \\ 0, & \hat{\sigma} = \hat{\sigma}_{\min} \text{ and } x < 0 \\ x, & \text{otherwise} \end{cases} \tag{31}$$

where $\hat{\sigma}$ is the estimated value of the $\sigma$, $\tilde{\sigma} = \sigma - \hat{\sigma}$ is the estimated error, $\Gamma$ is a positive design constant, and $x$ is an adaptive function [29].

$$\dot{\hat{\sigma}} = \Gamma \mathrm{Proj}\left(\hat{\sigma}, x\right) \tag{32}$$

The projection operator has the following conclusion for any adaptive function $x$.

$$\begin{cases} \hat{\sigma} \in \Omega_\sigma = \{\hat{\sigma}_{\min} \le \hat{\sigma} \le \hat{\sigma}_{\max}\} \\ \tilde{\sigma}\left[\mathrm{Proj}\left(\hat{\sigma}, x\right) - x\right] \le 0 \end{cases} \tag{33}$$

Substituting (29), (30) into (28), we can get

$$\dot{V}_1 = -k_1\varepsilon^2 \leq 0 \tag{34}$$

To eliminate the problem of computational expansion and controller saturation of virtual controller, a command filter is designed as

$$\begin{bmatrix} \dot{q}_1 \\ \dot{q}_2 \end{bmatrix} = \begin{bmatrix} q_2 \\ 2\xi\omega_n \left( S_R \left( \frac{\omega_n^2}{2\xi\omega_n} \left( S_M(u) - q_1 \right) \right) - q_2 \right) \end{bmatrix} \tag{35}$$

where $u = i_q^d$, $q_1 = i_q^c$, $\xi$ is the damping, $\omega_n$ is the bandwidth, $S_R(\cdot)$ is the rate limiting and $S_M(\cdot)$ is the amplitude limiting in Figure 2.

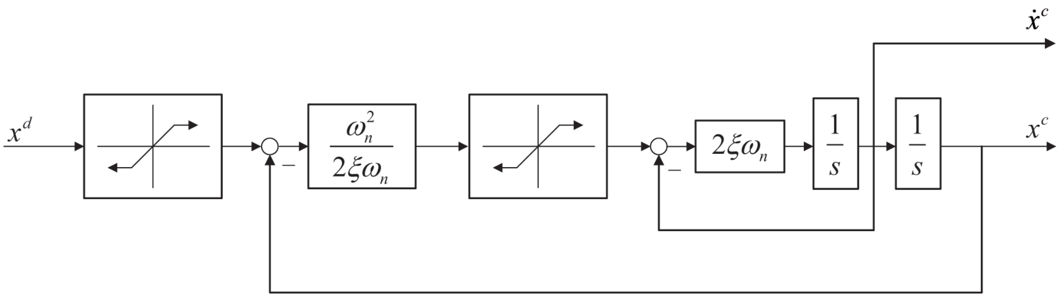


Figure 2. Structure of the constrained command filter

Although command filter solves the problems of computational expansion in the traditional backstepping controller, the command filter will produce a filtering error. In order to eliminate the influence of filtering error, a filtering compensation signal $\eta$ is introduced as

$$\eta = \varepsilon - \bar{\varepsilon} \tag{36}$$

$$\dot{\eta} = -k_1\eta + g\left(i_q^c - i_q^d\right) \tag{37}$$

where $k_1$ is a positive constant and $g = \frac{3\pi\psi_f n_p}{2\tau M} r$. According to (6), (19), (36), (37), the derivative equation for $\bar{\varepsilon}$ is calculated as

$$\begin{aligned} \dot{\bar{\varepsilon}} &= \dot{\varepsilon} - \dot{\eta} \\ &= -g\left(i_q^c - i_q^d\right) + \dot{\varepsilon} + k_1\eta \\ &= -g\left(i_q^c - \frac{2\tau M}{3\pi n_p \psi_f}\left(\frac{B}{M}v + \dot{v}^c - F + \frac{e_1\dot{\mu}}{\mu} - k_1\frac{\varepsilon}{r}\right)\right) + \dot{\varepsilon} + k_1\eta \\ &= -k_1\varepsilon + ge_2 - r\left(\dot{e}_1 - \frac{e_1\dot{\mu}}{\mu}\right) + \dot{\varepsilon} + k_1\eta \\ &= ge_2 - k_1\bar{\varepsilon} \end{aligned} \tag{38}$$

The second Lyapunov function is designed as

$$V_2 = \frac{1}{2}\bar{\varepsilon}^2 + \frac{1}{2}e_2^2 + \frac{1}{2}e_3^2 \tag{39}$$

Taking the derivative of $V_2$, yields

$$\dot{V}_2 = \bar{\varepsilon}\left(ge_2 - k_1\bar{\varepsilon}\right) + e_2\left(\frac{u_q}{L_q} - \frac{v\pi n_p\psi_f}{L_q\tau} - \frac{v\pi n_p i_d}{\tau} - \frac{R}{L_q}i_q - \dot{i}_q^c\right)$$

$$
\begin{aligned}
&+e_3\left(-\frac{R}{L_d}i_d+\frac{\pi n_p v i_q}{\tau}+\frac{u_d}{L_d}\right)\\
=&-k_1\bar{\varepsilon}^2+e_3\left(-\frac{R}{L_d}i_d+\frac{\pi n_p v i_q}{\tau}+\frac{U_d}{L_d}\right)\\
&+e_2\left(\frac{u_q}{L_q}-\frac{v\pi n_p\psi_f}{L_q\tau}-\frac{v\pi n_p i_d}{\tau}-\frac{R}{L_q}i_q-\dot{i}_q^c+g\bar{\varepsilon}\right)
\end{aligned}
\tag{40}
$$

The control law can be designed as

$$u_q=L_q\left(\frac{v\pi\psi_f n_p}{L_q\tau}+\frac{v\pi i_d n_p}{\tau}+\frac{Ri_q}{L_q}+\dot{i}_q^c+g\bar{\varepsilon}-k_2e_2\right) \tag{41}$$

$$u_d=L_d\left(\frac{Ri_d}{L_d}-\frac{\pi n_p v i_q}{\tau}-k_3e_3\right) \tag{42}$$

Substituting (41), (42) into (40), one obtains

$$\dot{V}_2=-k_1\bar{\varepsilon}^2-k_2e_2^2-k_3e_3^2\leq 0 \tag{43}$$

According to Lyapunov's theory, the asymptotic stability of the system is proved.

4. **Experimental Results.** To verify the effectiveness of the controller, some experiments are carry out in this section. PI, ABC and the proposed algorithm are respectively applied to PMLSM. PMLSM control platform based on dSPACE is established to carry out experiments on the control algorithm in Figure 3. The operating frequency of dSPACE1104 is 250 MHz, which is composed of PWM generator, encoder and 16 bit analog-to-digital converter (ADC) interface. The current signal is measured by Hall sensor, and the speed and position are measured by incremental encoder and sent to dSPACE. Three sets of IGBT intelligent power module (IPM) are used in the inverter, and the switching frequency of IPM is set to 5 KHz. In this paper, the sampling periods of speed loop and current loop are respectively 400 µs and 200 µs, and the dead time is set to 5 µs. The specific parameters of PMLSM are given in Table 1.

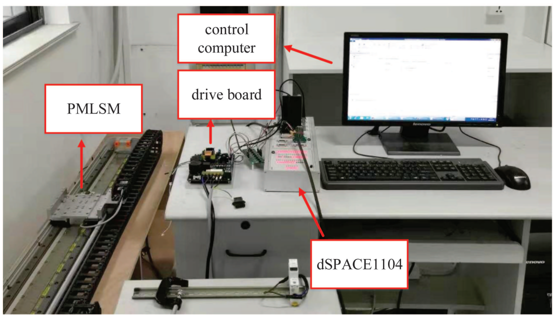


(a) Experimental platform setup

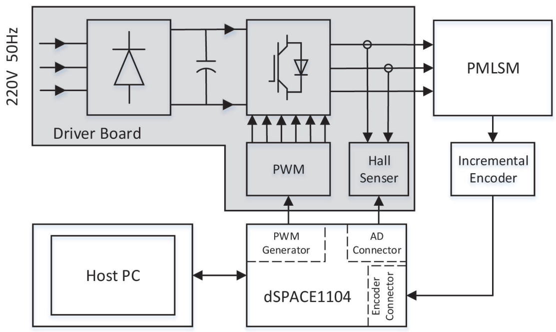


(b) Topology of experimental platform

FIGURE 3. Experimental system

In the experiment, the reference speed is given as 0.5 m/s. The parameters of the method are as follows: $k_1 = 10$, $k_2 = k_3 = 3000$, $\gamma_1 = 10$, $\mu_0 = 0.6$, $\mu_\infty = 0.06$, $d = 1$, $a = 10$, $\zeta = 0.5$, $\omega_n = 1000$.

The experimental results are shown in Figures 4-8. Figure 4 shows the speed response under three methods: The three methods have similar rise times, but the PI controller has the largest overshoot, followed by ABC, and this method has a smallest overshoot than the other two methods, due to the limitations of PPC. Besides, it can be found that

TABLE 1. Motor parameters

| Parameter | Symbol | Value |
|---|---|---|
| Resistance (Ω) | $R$ | 9.7 |
| Inductance (mH) | $L$ | 43.3 |
| Mover mass (kg) | $M$ | 3.2 |
| Frictional coefficient (Ns/m) | $B$ | 5 |
| Pole pith (m) | $\tau$ | 0.0263 |
| Permanent magnet flux (Wb) | $\varphi_f$ | 0.165 |
| Pole pairs | $n_p$ | 2 |

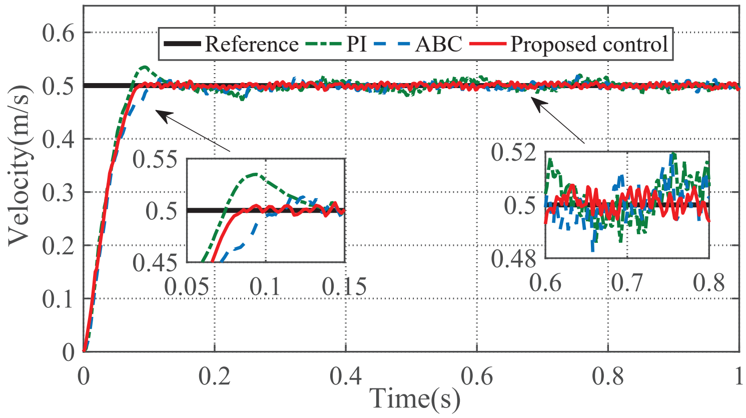


FIGURE 4. Comparison of speed curve under three methods

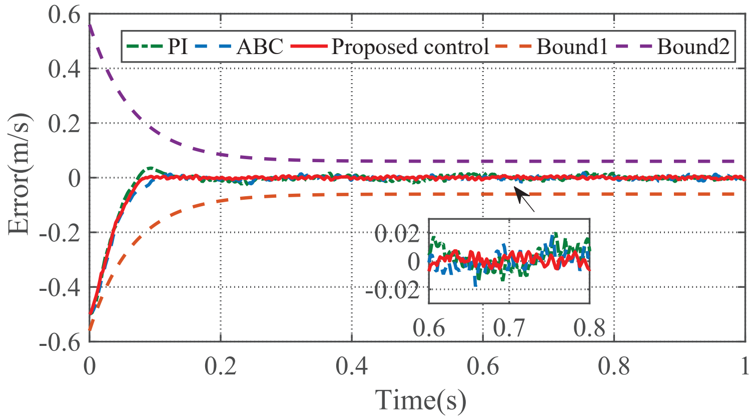


FIGURE 5. Speed tracking error under three methods

compared with the other two methods, the steady-state fluctuation of the permanent magnet linear synchronous motor applied by this method is smallest. The speed tracking error of a PMLSM under the three control methods is shown in Figure 5, and we can see the speed tracking error of the proposed method is within the PPF bounds.

Figure 6 shows the filtering effect and the signal compensation of the command filter, and the output signal $i_q^c$ can track the input signal $i_q^d$ effectively. By filtering the output of virtual control, the saturation problem of controller input is solved. Figure 7 shows the output of the RBF neural network disturbance observer, which is used to compensate the controller as feedforward signal. In Figure 8, experimental data of some parameters

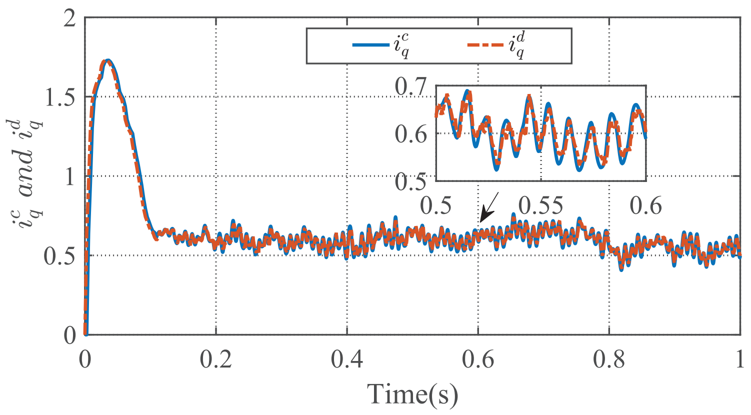


FIGURE 6. The filtering effect of the command filter

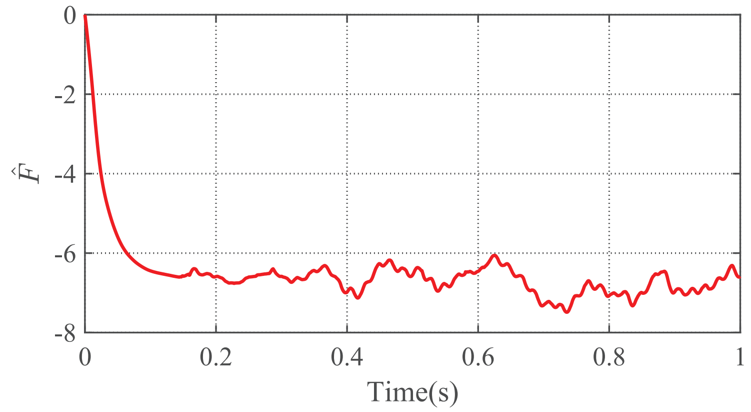


FIGURE 7. The output of RBF disturbance observer

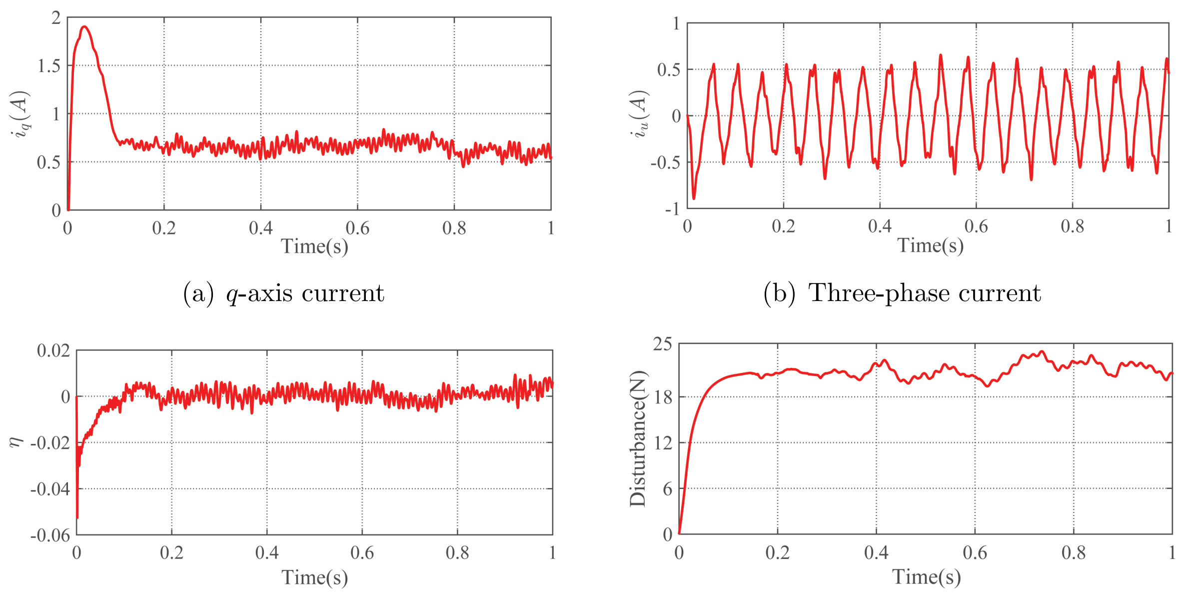


(a) $q$-axis current

(b) Three-phase current

(c) Signal compensation of the command filter

(d) Estimate disturbance

FIGURE 8. Some experimental performance under the proposed method

are provided. It can be seen, the compensation signal can well compensate the filtering error and the force ripple is serious which reduces the tracking performance, the force is between about 18 N and 25 N. By applying the proposed method, the tracking precision is improved. Detailed quantitative data of experiment for comparisons are given in Table 2. It can be seen that, the method we proposed shows better dynamic-state and steady-state performances. Its overshoot is much lower than the other two methods, and its setting time and max fluctuation are also much improved.

TABLE 2. Dynamic-state and steady-state performances in experiment

| Index | PI | ABC | Proposed |
|---|---|---|---|
| Overshoot (%) | 6.96 | 2.56 | 0.24 |
| Setting time (s) | 0.142 | 0.135 | 0.097 |
| Max fluctuation (m/s) | 0.035 | 0.023 | 0.012 |

5. **Conclusion.** In this paper, a prescribed performance based adaptive neural backstepping is proposed for PMLSM control. Firstly, by using the prescribed performance function, the tracking error of the system is limited within a prescribed range, and the steady-state fluctuation of the system is reduced. Secondly, the disturbance is observed by neural network and compensated as feedforward signal, which improves the dynamic and steady performance of the system. Then, a command filter is introduced to eliminate the computational expansion and control saturation of the controller. Finally, experimental results show that this method has better robustness and steady-state performance than other control methods. For the future study, the research direction is to optimize the command filter to generate compensation signals with smaller force ripple and improve the tracking performance.

**Acknowledgment.** This work is partially supported by the National Natural Science Foundation of China (Grant No. 62222307, No. 61973140) and the Natural Science Foundation of Jiangsu Province (Grant No. BK20211235). The authors also appreciatively acknowledge the helpful suggestions and comments of the reviewers, which have enhanced the presentation.

**REFERENCES**

[1] H. Wang, J. Li, R. Qu, J. Lai, H. Huang and H. Liu, Study on high efficiency permanent magnet linear synchronous motor for maglev, *IEEE Transactions on Applied Superconductivity*, vol.28, no.3, pp.1-5, 2018.

[2] S. G. Lee, S. A. Kim, S. Saha, Y. W. Zhu and Y. H. Cho, Optimal structure design for minimizing detent force of PMLSM for a ropeless elevator, *IEEE Transactions on Magnetics*, vol.50, no.1, pp.1-4, 2014.

[3] K. Wang, Z. Deng, L. Shi, Q. Ge and Y. Li, Traction control of multi-section long primary ironless linear synchronous motor for maglev vehicle, *2019 12th International Symposium on Linear Drives for Industry Applications (LDIA)*, pp.1-4, 2019.

[4] M. Wang, L. Li and D. Pan, Detent force compensation for PMLSM systems based on structural design and control method combination, *IEEE Transactions on Industrial Electronics*, vol.62, no.11, pp.6845-6854, 2015.

[5] M. Wang, L. Li, D. Pan, Y. Tang and Q. Guo, High-bandwidth and strong robust current regulation for PMLSM drives considering thrust ripple, *IEEE Transactions on Power Electronics*, vol.31, no.9, pp.6646-6657, 2016.

[6] Z. Deng, K. Wang and L. Zhao, Research on the changeover strategy of multi-section long primary linear synchronous motor for maglev vehicle, *2019 22nd International Conference on Electrical Machines and Systems (ICEMS)*, pp.1-5, 2019.

[7] M. Wang, R. Yang, C. Zhang, J. Cao and L. Li, Inner loop design for PMLSM drives with thrust ripple compensation and high-performance current control, *IEEE Transactions on Industrial Electronics*, vol.65, no.12, pp.9905-9915, 2018.

[8] S. J. Kim, E. J. Park, S. Y. Jung and Y. J. Kim, Optimal design of reformed auxiliary teeth for reducing end detent force of stationary discontinuous armature PMLSM, *IEEE Transactions on Applied Superconductivity*, vol.26, no.4, pp.1-5, 2016.

[9] Z. Zhang, R. Ma, L. Wang and J. Zhang, Novel PMSM control for anti-lock braking considering transmission properties of the electric vehicle, *IEEE Transactions on Vehicular Technology*, vol.67, no.11, pp.10378-10386, 2018.

[10] D. Hu, W. Xu, R. Dian, Y. Liu and J. Zhu, Loss minimization control of linear induction motor drive for linear metros, *IEEE Transactions on Industrial Electronics*, vol.65, no.9, pp.6870-6880, 2018.

[11] F. J. Lin, P. H. Shieh and P. H. Chou, Robust adaptive backstepping motion control of linear ultrasonic motors using fuzzy neural network, *IEEE Transactions on Fuzzy Systems*, vol.16, no.3, pp.676-692, 2008.

[12] M. Morawiec, The adaptive backstepping control of permanent magnet synchronous motor supplied by current source inverter, *IEEE Transactions on Industrial Informatics*, vol.9, no.2, pp.1047-1055, 2013.

[13] D. Xu, W. Zhang, P. Shi and B. Jiang, Model-free cooperative adaptive sliding-mode-constrained-control for multiple linear induction traction systems, *IEEE Transactions on Cybernetics*, vol.50, no.9, pp.4076-4086, 2020.

[14] R. Zhang, B. Xu, Q. Wei, P. Zhang and T. Yang, Harmonic disturbance observer-based sliding mode control of MEMS gyroscopes, *ISCIENCE CHINA: Information Sciences*, 2020.

[15] X. Yuan, Y. Wang, W. Sun and L. Wu, RBF networks-based adaptive inverse model control system for electronic throttle, *IEEE Transactions on Control Systems Technology*, vol.18, no.3, pp.750-756, 2010.

[16] Z. Peng, D. Wang and T. Li, Predictor-based neural dynamic surface control for distributed formation tracking of multiple marine surface vehicles with improved transient performance, *SCIENCE CHINA: Information Sciences*, vol.59, no.9, 092210, 2016.

[17] D. Xu, J. Huang, X. Su and P. Shi, Adaptive command-filtered fuzzy backstepping control for linear induction motor with unknown end effect, *Information Sciences*, vol.477, pp.118-131, 2019.

[18] J. Y. Lau, W. Liang and K. K. Tan, Motion control for piezoelectric-actuator-based surgical device using neural network and extended state observer, *IEEE Transactions on Industrial Electronics*, vol.67, no.1, pp.402-412, 2020.

[19] Q. Liu, D. Xu, B. Jiang and Y. Ren, Prescribed-performance-based adaptive control for hybrid energy storage systems of battery and supercapacitor in electric vehicles, *International Journal of Innovative Computing, Information and Control*, vol.16, no.2, pp.571-583, 2020.

[20] W. Chen, S. S. Ge, J. Wu and M. Gong, Globally stable adaptive backstepping neural network control for uncertain strict-feedback systems with tracking accuracy known a priori, *IEEE Transactions on Neural Networks and Learning Systems*, vol.26, no.9, pp.1842-1854, 2015.

[21] N. Lu, X. Sun and X. Zheng, Command filtered adaptive fuzzy backstepping fault-tolerant control against actuator fault, *ICIC Express Letters*, vol.15, no.4, pp.357-365, 2021.

[22] Z. Peng and J. Wang, Output-feedback path-following control of autonomous underwater vehicles based on an extended state observer and projection neural networks, *IEEE Transactions on Systems, Man, and Cybernetics: Systems*, vol.48, no.4, pp.535-544, 2018.

[23] S. Wang, X. Ren, J. Na and T. Zeng, Extended-state-observer-based funnel control for nonlinear servomechanisms with prescribed tracking performance, *IEEE Transactions on Automation Science and Engineering*, vol.14, no.1, pp.98-108, 2017.

[24] C. P. Bechlioulis and G. A. Rovithakis, Robust adaptive control of feedback linearizable MIMO nonlinear systems with prescribed performance, *IEEE Transactions on Automatic Control*, vol.53, no.9, pp.2090-2099, 2008.

[25] L. Zhang and G. H. Yang, Adaptive fuzzy prescribed performance control of nonlinear systems with hysteretic actuator nonlinearity and faults, *IEEE Transactions on Systems, Man, and Cybernetics: Systems*, vol.48, no.12, pp.2349-2358, 2018.

[26] X. Shao, Q. Hu, Y. Shi and B. Jiang, Fault-tolerant prescribed performance attitude tracking control for spacecraft under input saturation, *IEEE Transactions on Control Systems Technology*, vol.28, no.2, pp.574-582, 2020.

[27] J. Na, Q. Chen, X. Ren and Y. Guo, Adaptive prescribed performance motion control of servo mechanisms with friction compensation, *IEEE Transactions on Industrial Electronics*, vol.61, no.1, pp.486-494, 2014.
[28] Z. Wang, C. Hu, Y. Zhu, S. He, K. Yang and M. Zhang, Neural network learning adaptive robust control of an industrial linear motor-driven stage with disturbance rejection ability, *IEEE Transactions on Industrial Informatics*, vol.13, no.5, pp.2172-2183, 2017.
[29] D. Xu, X. Song, W. Yan and B. Jiang, Model-free adaptive command-filtered-backstepping sliding mode control for discrete-time high-order nonlinear systems, *Information Sciences*, vol.485, pp.141-153, 2019.

## Author Biography

**Li Zhang** received the Ph.D. degree in instruments and apparatuses from the University of Aeronautics and Astronautics, Nanjing, China, in 2012. He was a Visiting Fellow at Pennsylvania State University, in 2010. He is currently a Lecturer with the Nanjing Institute of Technology. His research interests include adaptive control, synthetic jet and embedded system.

**Jinlei Pei** received the B.S. degree in electrical engineering and automation from Hainan University, Haikou, China in 2018. He is currently working toward the Ph.D. degree in control engineering with Jiangnan University, Wuxi, China. His current research interests include fault diagnosis and fault-tolerant control, multi-agent systems and smart grid.

**Tinglong Pan** received his B.Eng. degree in industrial automation from China University of Mining and Technology, Xuzhou, China, in 1999, and the Ph.D. degree in power electronics and power drive from China University of Mining and Technology, Xuzhou, China, in 2004.

He is currently a Professor at Jiangnan University, where his research interests include microgrid control technology, power conversion technology, power drive system and its intelligent control technology.

**Weilin Yang** received his B.Eng. degree in machine design & manufacture and their automation from University of Science and Technology of China, Hefei, China, in 2009, and the Ph.D. degree in mechanical engineering from City University of Hong Kong, Hong Kong, in 2013.

He was a postdoctoral researcher at Masdar Institute of Science and Technology (now Khalifa University), Abu Dhabi, UAE, 2013-2016. He was a research engineer of General Electric (GE) Global Research, Shanghai, 2016-2017. He joined Jiangnan University in July 2017, where he is currently an Associate Professor. His research interests include modeling and control of energy systems, robust model predictive control, and dada-driven control.

**Dezhi Xu** received the Ph.D. degree in control theory and control engineering from Nanjing University of Aeronautics and Astronautics, China, in 2013.

He was a Visiting Fellow with the Department of Biomedical Engineering, City University of Hong Kong, China, from 2018 to 2019. He is currently a Professor and Doctoral Supervisor with the Jiangnan University. His research interests include data-driven control, fault diagnosis and fault-tolerant control, multi-agent systems and cyber-physical systems, technologies of renewable energy, motor control, and smart grid. Prof. Xu was supported by the National Natural Science Fund for Excellent Young Scientists Fund Program in 2022. He was a recipient of the First Class Prize of Science and Technology Progression from the China General Chamber of Commerce in 2016, and the Best Young Scholar of Jiangnan University in 2022. He was a Guest Editor for the *International Journal of Innovative Computing, Information and Control* and the *Electric Power*. He currently serves as an Editorial Board Member for the *International Journal of Innovative Computing, Information and Control*, the *Electric Power*, the *Electrotechnical Application* and the *Electrical Engineering*. He is a Committee Member of the Association of Energy Internet, and Trusted Control in Chinese Association of Automation (CAA), and the Energy Storage in China Renewable Energy Society (CRES).